Rapid droplet mixers for digital microfluidic systems†

Phil Paik,* Vamsee K. Pamula* and Richard B. Fair

*Department of Electrical Engineering, Duke University, Durham, North Carolina 27708,
USA. E-mail: pyp@ee.duke.edu; vkp@ee.duke.edu*

The mixing of analytes and reagents for a biological or chemical lab-on-a-chip is an important, yet difficult, microfluidic operation. As volumes approach the sub-nanoliter regime, the mixing of liquids is hindered by laminar flow conditions. An electrowetting-based linear-array droplet mixer has previously been reported. However, fixed geometric parameters and the presence of flow reversibility have prevented even faster droplet mixing times. In this paper, we study the effects of varying droplet aspect ratios (height : diameter) on linear-array droplet mixers, and propose mixing strategies applicable for both high and low aspect ratio systems. An optimal aspect ratio for four electrode linear-array mixing was found to be 0.4, with a mixing time of 4.6 seconds. Mixing times were further reduced at this ratio to less than three seconds using a two-dimensional array mixer, which eliminates the effects of flow reversibility. For lower aspect ratio ($\leq$0.2) systems, we present a split-and-merge mixer that takes advantage of the ability to perform droplet splitting at these ratios, resulting in a mixing time of less than two seconds.

1 Introduction

Mixing is an important microfluidic operation in many biological and chemical μTAS (micro total analysis systems) or lab-on-a-chip applications. The rapid mixing of liquids using a minimum device area allows for a high throughput system where hundreds of samples can be quickly processed and analyzed on a single chip. However, as microfluidic devices approach sub-nanoliter scales, the ability to rapidly mix liquids is hindered by reduced volume flow rates and very low Reynolds numbers. Mixing can be improved by creating turbulent flows or by creating multilaminates to achieve faster mixing rates *via* diffusion. Since turbulent flow often requires liquids to travel at high velocities, research in both continuous-flow and droplet-based mixers have focused on the latter principle. We have recently reported that while creating multilaminates, care should also be taken to reduce the effects of flow reversibility.[1] In a flow-reversible mixer, complex multi-laminates are reverted to their original, simpler configurations, which ultimately slow the mixing process. Hence, the mitigation or elimination of flow reversible effects is crucial for mixing in systems with non-continuous flow, *i.e.* droplet-based systems.

Droplet-based microfluidic systems differ from continuous flow systems in that they manipulate discrete droplets rather than continuous liquid streams. They possess a number of advantages over continuous-flow systems, such as the ability to control each droplet independently, enabling complex procedures to be performed in a manner similar to traditional benchtop protocols. Reconfigurable flow and the absence of permanently etched channels also allows for a highly integrated, scalable and flexible architecture.

While a number of researchers have demonstrated the ability to transport, dispense, merge and split droplets through various methods,[2–8] only a few droplet-based mixers have been studied to date. Mixing can be achieved either by passive or active means. Passive mixing is mediated purely through diffusion without any external energy for the process, whereas active mixing takes advantage of external energy, through actuation of some sort, to create either dispersed multilaminates or turbulence within the droplet. Hosokawa *et al.* have demonstrated the ability to form droplets using a hydrophobic microcapillary valve device and later transported, merged and actively mixed the droplets with the help of air pressure.[3] Meanwhile, our group and others have demonstrated devices which manipulate droplets *via* electric fields.[4–8] We have previously reported a passive droplet mixer, where the droplets are actuated to coalesce only using an array of electrodes to actuate the droplets through electrowetting.[9] More recently, we have demonstrated an active droplet mixer using the same system, where coalesced droplets are oscillated among a linear array of electrodes.[1] Fowler *et al.* have also claimed fast droplet mixing using similar electrowetting actuation to roll coalesced droplets in order to double the number of interfacial layers.[10]

While Fowler *et al.* and Hosokawa *et al.* observed mixing from the top view only, we observed both passive and active mixing using simultaneous top and side profile imaging techniques. We have demonstrated in Pamula *et al.*[9] that observing the mixing process from just the top view can lead to erroneous conclusions about the mixing times. Simultaneous top and side views allow us to better visualize the mixing process as well as obtain a more accurate assessment of mixing times. For example, we were able to clearly visualize the flow-reversible nature of our linear array active mixer, due to an oscillatory mixing scheme similar to that used by Hosokawa *et al.*. Ideally, a tomographical view of the droplets while being mixed would yield more detailed information about the evolution of the mixing process and the homogeneity of mixing.[11]

In this paper, we study the effects of varying an important geometric parameter in droplet-based systems on linear array mixing, aspect ratio, which is defined as the ratio of the gap height to the electrode pitch size. For a lab-on-a-chip that is required to perform dispensing, transport, mixing, and splitting, it is important to study this effect on mixing, since the aspect ratio plays an important role in performing droplet formation and splitting.[12] Based on these results, we then present various mixing schemes for different system geometries. For low aspect ratio systems, we demonstrate rapid mixing by incorporating droplet splitting. In higher aspect ratio systems, we eliminate

the effects of flow reversibility in order to improve mixing times by using various two-dimensional array mixing schemes. As a result, we offer two new mixing strategies which can facilitate important applications ranging from kinetic assays used to detect biological or chemical agents, to fast multiple dilutions of biological and chemical sample droplets, where repeated mixing and splitting operations are required.[13,14]

2 Experimental

Chip fabrication

The setup consists of two parallel plates between which droplets of polarizable and/or conductive liquid are sandwiched, as shown in Fig. 1. The bottom plates were fabricated using standard microfabrication techniques. The bottom glass plate consists of an array of independently addressable control electrodes patterned in a 200 nm thick layer of chrome, which is further coated with Parylene C (800 nm) for insulation. The top glass plate is coated with a conducting layer of optically transparent indium tin oxide (ITO) to form the ground electrode. Both top and bottom plates are coated with a thin hydrophobic layer of Teflon AF 1600 (50 nm). A glass spacer is used to separate the top and bottom plates, yielding a fixed gap. More details on the electrowetting experimental setup have been reported elsewhere.[4]

Operation of the microfluidic device

Droplets are actuated through electrowetting in which the interfacial tension of the droplets is modulated with voltage.[5] The volume of the droplet is chosen to ensure an overlap between the droplet and adjacent electrodes. Filler fluid of immiscible 1cSt silicone oil is used to surround the droplet to prevent evaporation and reduce the droplet actuation voltage. A custom electronic controller was built to address and switch each electrode independently.

The basic scheme for mixing is shown in top and side views in Fig. 1. A fluorescent droplet is initially actuated towards a stationary non-fluorescent droplet until they are coalesced. Then, active mixing is initiated, where the merged droplet is transported over a number of electrodes at various frequencies depending on the mixing scheme. The actuation voltage used for all experiments is 50 V, unless stated otherwise. Fluorescence was chosen for better visualization and higher sensitivity. The fluorescent droplets (F) contain 1 mM fluorescein (JT Baker), 0.125 M KCl to make the droplet conductive, and 0.125 M NaOH to maintain the proper pH for fluorescence. Controlled experiments have shown that constant fluorescence levels were maintained for at least five minutes in a fluorescent droplet oscillated over several electrodes at this concentration. The non-fluorescent (NF) droplets contain 0.125 M KCl and 0.125 M NaOH only. The interfacial tension of the F droplet with respect to 1 cSt silicone oil was 37 dynes cm^{-1} whereas the NF droplet was 36 dynes cm^{-1} with the same oil. The viscosity for the F and NF droplets was 1.396 and 1.373 cP, and the conductivity was 29.7 mMho and 25.9 mMho, respectively.

Droplet visualization

It has been previously shown that both top and side profiles of the droplet must be viewed in order to properly assess mixing times.[9] Two cameras are used in all the experiments to simultaneously view the top and side views of the droplet. The fluorescent droplets are excited using a tungsten lamp with a blue filter (490 nm). Both cameras are mounted with long pass filters (>510 nm) to collect the fluorescence. The videos are later digitized at 30 frames per second with the top and side views perfectly synchronized. All experiments are recorded well beyond a subjective assessment of mixing time for later analysis.

Image processing

A custom-written program using the image processing toolkit in MATLAB is used to obtain an objective assessment of mixing times. A snapshot of the completely mixed droplet at the end of the digitized mixing video file is obtained. This snapshot is an image of the completely mixed droplet, and is used as an internal reference. Every frame from the start of mixing is then compared to this mixed droplet reference frame by subtracting the two images. A histogram of this difference allows us to determine the percentage of the droplet that is mixed. An arbitrary threshold of 95 percent is used to acquire a final mixing time. All experiments revealed the side view appearing completely mixed much earlier than the top view. Hence, only images from the top view are shown in the results.

3 Results and discussion

Effects of aspect ratio on linear array mixing

The effect of varying aspect ratios on droplet mixing was investigated using a 1.5 mm electrode pitch size. For each case, the volumes of both the F and the NF droplets were adjusted to maintain a constant droplet diameter. Fig. 2 shows the results using a four-electrode linear array mixer with a switching frequency of 16 Hz. The switching frequency denotes the amount of time an electrode is ON. The fastest mixing time achieved was with an aspect ratio of 0.4. Lower aspect ratios resulted in an almost linear increase in mixing times, while higher aspect ratios resulted in marginally worse performance. The parameters for each experiment are summarized in Table 1.

For very low aspect ratio systems (<0.4), we observed the absence of complex flow patterns as seen in previous experiments. The decreased gap heights inhibit vertical flow (i.e. flow from the bottom to the top of a droplet) from fully circulating, resulting in worse mixing times. These differences in flow patterns are shown in Fig. 3, where droplets were mixed on a four-electrode linear array mixer using gap heights of 600 μm and 300 μm, resulting in aspect ratios of (a) 0.4 and (b) 0.2. The volumes of the coalesced droplets are 2.64 μl and 1.36 μl, respectively. Each image was taken 1.2 seconds after coalescence. At an aspect ratio of 0.4, flow within the droplet is distributed within its entire area as seen in Fig. 3a. By contrast,
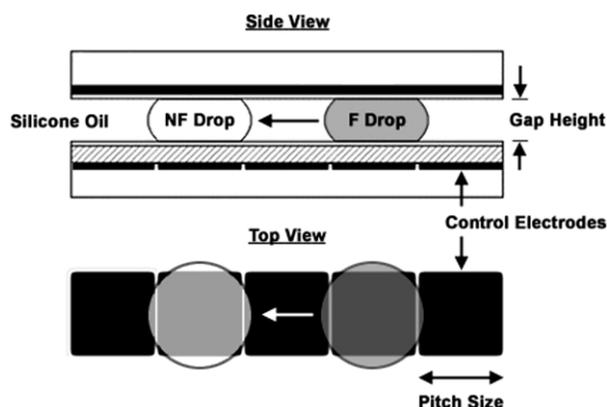
Fig. 1 Schematic side and top view of the electrowetting-based droplet mixer.

a lower aspect ratio results in much of the F droplet isolated from the NF side throughout the mixing process, as seen in Fig. 3b. Hence, mixing does not benefit as it would from the more complex and uniformly distributed flow patterns generated in a system with a larger spacing.

In systems where the aspect ratios are higher than the optimal value, the slight increase in mixing times is due to larger droplet volumes. The flow patterns generated by these systems were comparable to those of the optimal system, however, the increased volume would require more time for the diffusion process to complete as diffusion lengths have now increased.

Split-and-merge mixing

The mixing of two 800 nl droplets at an aspect ratio of 0.2 in the mixer described above took 14.9 seconds to complete, which is three times slower than mixing at the optimal ratio of 0.4. It has been reported that the threshold below which splitting can occur

is also 0.2.[4,12] This suggests that applications requiring splitting operations (*i.e.* division of samples and multiple dilutions of samples) would be hindered by slow mixing. Thus, alternative mixing strategies need to be explored for these low aspect ratio systems. By introducing a split-and-merge mixer, we propose a scheme where this very same splitting will be used to enhance the efficiency of mixing.

The ability to split a coalesced droplet into smaller droplets allows for a number of mixing schemes. For example, separate mixing operations can be performed to completeness on each smaller droplet, or droplets can be split, oscillated, remerged, and split again. A simple three-electrode split-and-merge mixer is shown in Fig. 4.

A coalesced droplet was oscillated once over three electrodes before being split into two. The smaller droplets were then remerged one cycle later, and this process was repeated until mixing was complete. The switching frequency used was 16 Hz, and the volume of each droplet was 800 nl. A voltage of 80 V was required to successfully split the droplet. Fig. 5 shows a
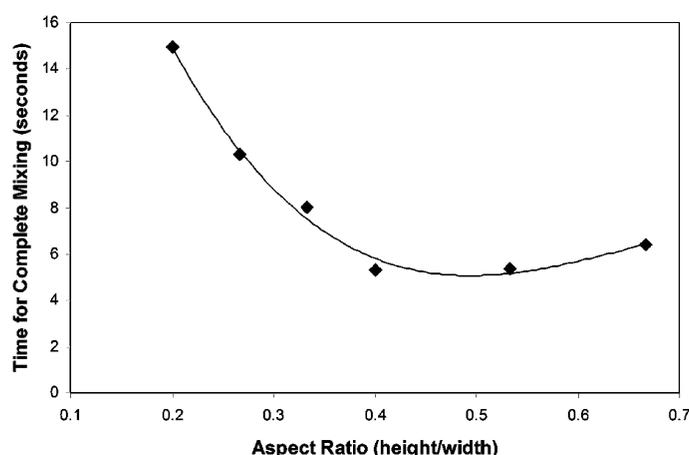
Fig. 2 Performance of four-electrode linear array mixers at 16 Hz switching frequencies with various aspect ratios. Note: the solid line is included for visualization purposes and is not meant to represent any curve fit.

Table 1 Mixing times and geometries for various rapid droplet mixers

	Electrode pitch	Gap height	Aspect ratio	Volume	Mixing time
4-electrode linear array	1.5 mm	1.0 mm	1 : 1.5 (0.66)	2350 nl	6.4 s
4-electrode linear array	1.5 mm	800 µm	1 : 1.88 (0.53)	1866 nl	5.4 s
4-electrode linear array	1.5 mm	600 µm	1 : 2.5 (0.40)	1400 nl	4.6 s
4-electrode linear array	1.5 mm	500 µm	1 : 3.0 (0.33)	1166 nl	8.1 s
4-electrode linear array	1.5 mm	400 µm	1 : 3.75 (0.27)	950 nl	10.3 s
4-electrode linear array	1.5 mm	300 µm	1 : 5.0 (0.20)	800 nl	14.9 s
3-electrode split and merge	1.5 mm	300 µm	1 : 5.0 (0.20)	800 nl	1.7 s
2 × 2 electrode array	1.5 mm	600 µm	1 : 2.5 (0.40)	1400 nl	9.95 s
2 × 3 electrode array	1.5 mm	600 µm	1 : 2.5 (0.40)	1400 nl	6.1 s
2 × 4 electrode array	1.5 mm	600 µm	1 : 2.5 (0.40)	1400 nl	2.9 s
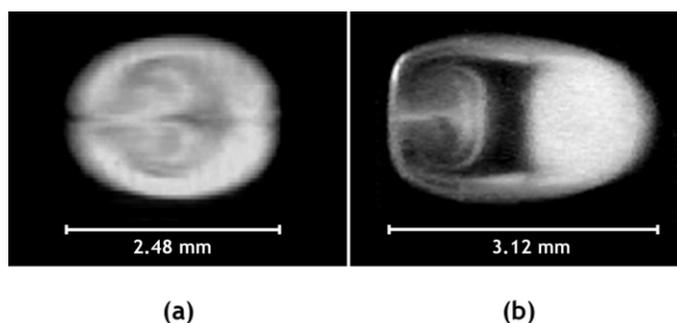
Fig. 3 Top view of four-electrode mixing in a system with aspect ratios of (a) 0.4 and (b) 0.2 at 1.2 seconds into mixing. The switching frequency used was 16 Hz.

sequence of time-lapsed images where a coalesced droplet just before and after splitting is shown on each row. It can be seen from these images that splitting and remerging resulted in a more homogenous droplet. By the end of the third split and merge sequence, the droplet appears nearly completely mixed. Complete mixing was achieved within 1.7 seconds.

2 × 2 Array mixing

In applications which require an aspect ratio greater than 0.2, the optimal ratio of 0.4 should be used. The mixing of two 1.4 μl droplets on a four-electrode linear array at this aspect ratio was complete within 4.6 seconds, given a 16 Hz switching frequency. It has been previously suggested that the presence of flow reversibility most likely prevents mixing from completing faster.[1] The unfolding of more complex flow patterns into simpler ones due to flow reversibility should be eliminated in

order to achieve even faster mixing times. One method to accomplish this is to use a larger number of electrodes in a linear-array design. When a coalesced droplet is oscillating among a set of electrodes, flow developed by any forward motion is countered by a backward motion. The effects of bi-directional motion can be mitigated by using more electrodes. However, in order to minimize the device area used for mixing, we have limited our previous experiments to only four electrodes.

An alternative method to achieve unidirectional motion is to move a coalesced droplet in a circular motion. This requires the mixing platform to be extended to two dimensions, the simplest of which is a 2 × 2 array of electrodes, as shown in the top row of Fig. 7.

Mixing times were obtained for 1, 2, 4, 8, and 16 Hz switching frequencies. The pitch size of each square electrode is 1.5 mm, and the gap height used is 600 μm. Square electrodes were used over interdigitated electrodes to simplify chip fabrication; however, mixing performance does not vary across
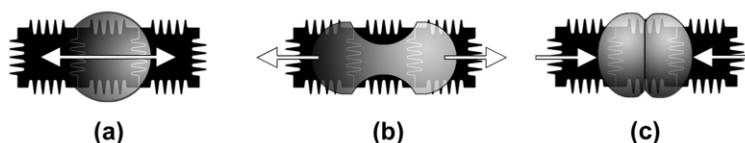
Fig. 4 Three-electrode mixing *via* split-and-merge. (a) A merged droplet is transferred across the three electrodes at 16 Hz. (b) The droplet is then split into two droplets and then remerged (c) at the same 16 Hz frequency.
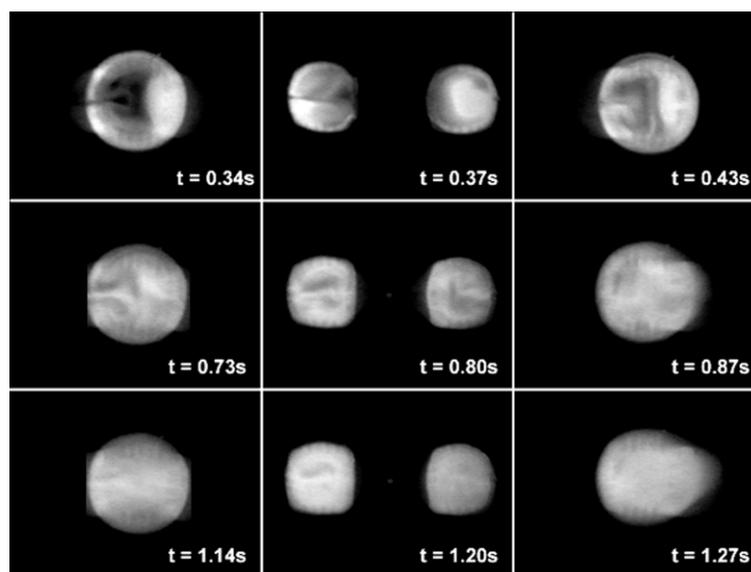
Fig. 5 Time-lapsed images of the top view of a droplet during three-electrode mixing at 16 Hz with splitting and merging.
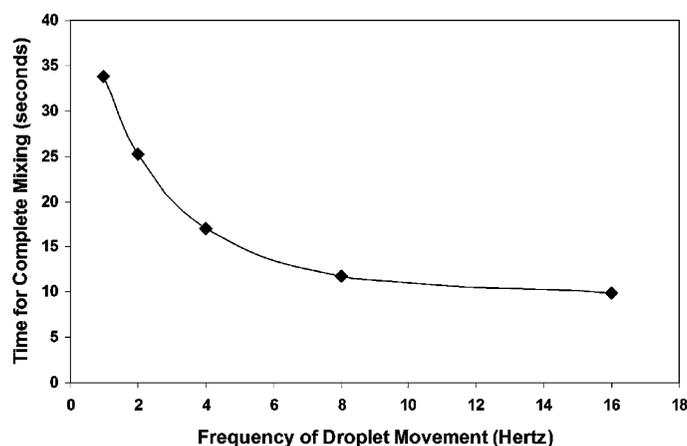
Fig. 6 Active mixing times as a function of switching frequency on a 2 × 2 electrode array. Note: the solid line is included for visualization purposes and is not meant to represent any curve fit.

the different shapes. The volume of each droplet is 1.4 μl. Fig. 6 shows that increasing the switching frequency results in faster mixing times. The fastest mixing time achieved was 9.95 seconds at 16 Hz.

Despite the elimination of flow reversible effects due to the unidirectional motion of the coalesced droplet, mixing on the 2 × 2 electrode array does not perform better than the four electrode linear array mixer. Fig. 7 shows a time-lapsed sequence of images from the top-view in a 2 × 2 electrode array experiment at 16 Hz. Each column represents the droplet in the same position with the same direction of motion on the array but in a different mixing cycle. Each row represents the droplet in motion within the same cycle in the mixing process. This allows us to observe droplet profiles on a specific electrode as a function of time.

It can be seen from each of the images in Fig. 7 that there exists a portion of the droplet that remains unmixed. We believe that this is caused by the fact that the coalesced droplet pivots around the center of the 2 × 2 electrode mixer, as indicated by

the white dots on the top row of Fig. 7. The flow patterns that are created when rotating about this common point prevent the fluorescent droplet from mixing with the center of the coalesced droplet. This unmixed area gradually becomes smaller as surrounding instabilities facilitate diffusion across this area.

2 × 3 Array mixing

To eliminate the problems associated with a static pivot point in 2 × 2 array mixing, coalesced droplets should instead be turning about a moving pivot point. The unmixed region formed in the 2 × 2 array can be eliminated if a translation is incorporated into the mixing scheme. The simplest case is with a 2 × 3 array mixer where a droplet now turns around two pivot points with one translational step in between, as shown in the top row of Fig. 8.

An average mixing time of 6.1 seconds was achieved at 16 Hz by rotating the droplet counter-clockwise in the 2 × 3 array
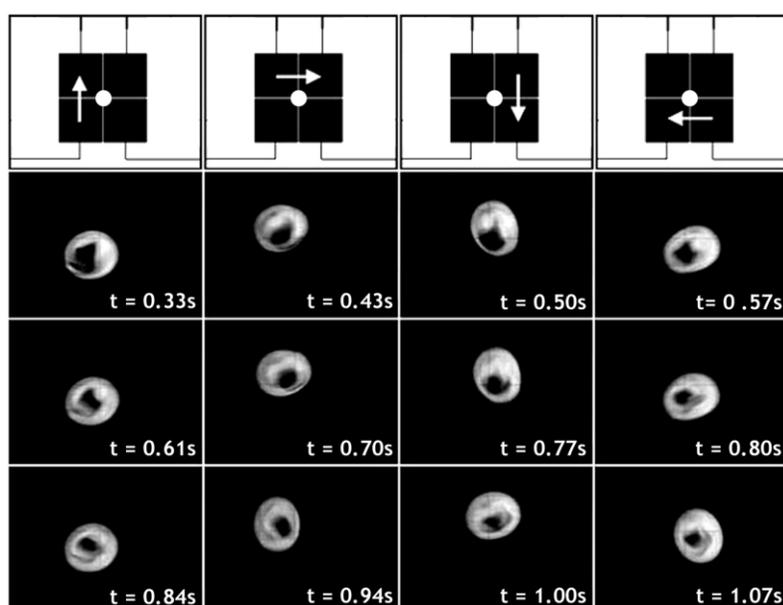
Fig. 7 Pivot point about which a droplet moves in a 2 × 2 mixer (top row) and time-lapsed images of 2 × 2 electrode mixing at 16 Hz.
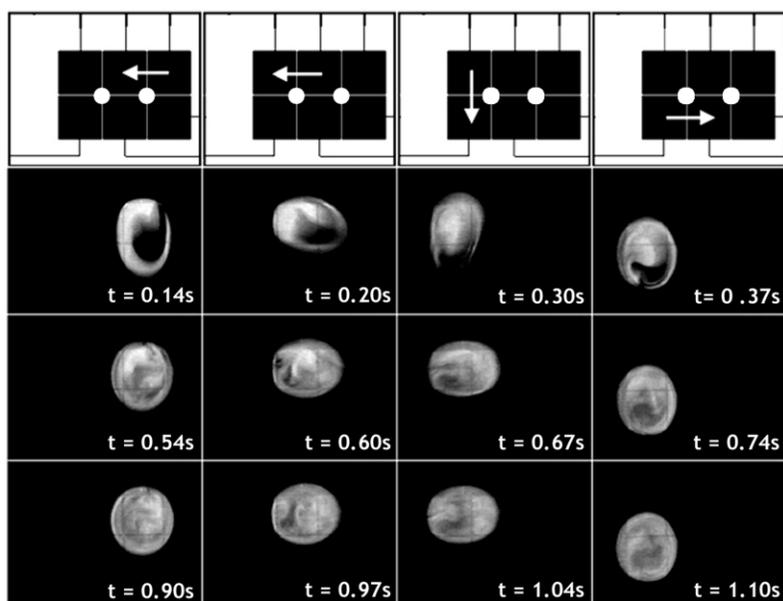
Fig. 8 Pivot point about which a droplet moves in a 2 × 3 mixer (top row) and time-lapsed images of 2 × 3 electrode mixing at 16 Hz. Four of six possible positions are shown.

mixer. This improved performance over the 2 × 2 array mixer is due to the additional translations between the pivot points, which allows for the flow patterns to develop within the droplet. Fig. 8 shows a sequence of time-lapsed images from a 2 × 3 array mixing experiment. By comparing the images within each column, we observe that the flow patterns take on very different forms after the droplet has completed one loop around the mixer. This suggests that the effects of flow reversibility no longer exist with a 2 × 3 array mixer as observed with previous linear mixing studies. Furthermore, we observe that the unmixed region caused by a static pivot point in the 2 × 2 array mixer is not sustained in a 2 × 3 array mixer. The result is a coalesced droplet which creates far more intricate flow patterns than previously observed.

2 × 4 Array mixing

While the presence of an electrode between the pivot points of a 2 × 3 array mixer significantly enhances mixing over a 2 × 2 array mixer, performance was still found to be worse than a four-electrode linear array mixer. This suggests that increasing the number of electrodes in one direction appears to have a greater effect on mixing than extending the mixer to another dimension such as 2 × 2. Thus, in order to maintain the absence of flow reversible effects and complexity of the 2 × 3 array mixer, yet still outperform the mixing rates of a four-electrode linear array mixer, a 2 × 4 array mixer was used.

A 2 × 4 array mixer has three possible pivot points, with up to two translations in between, as shown in the top row of Fig. 9. This adds an extra degree of flexibility over the 2 × 3 array mixer, as there are now a number of possible paths to perform mixing, two of which are shown in Fig. 10. Furthermore, the additional translation allows for flow patterns similar to the four-electrode linear array mixer to develop.

The lowest mixing time achieved using a 2 × 4 array mixer was 2.9 seconds at 16 Hz using the mixing scheme shown in Fig. 10b. A sequence of time-lapsed images for this mixing scheme can be seen in Fig. 9. Due to the absence of flow reversible effects and the additional translation, we see that no two images show droplets that share a common flow pattern. These flow patterns appear to be far more complex than the linear array, 2 × 2, or 2 × 3-array mixers, allowing mixing to proceed more efficiently. A similar mixing time of 2.9 seconds was also achieved with the scheme shown in Fig. 10a.

An alternative improvement to the 2 × 3 array mixer studied contained two additional pivot points rather than two additional translation steps as in the 2 × 4 array mixer. This pseudo 3 × 3 array mixer is shown in Fig. 11, where a coalesced droplet travels across eight electrodes in a unidirectional fashion. Each
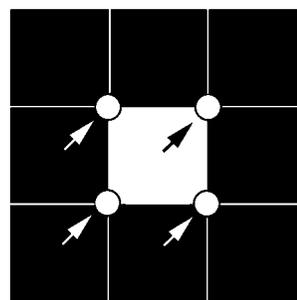
Fig. 11 Pivot points about which a droplet moves in a pseudo 3 × 3 array mixer.
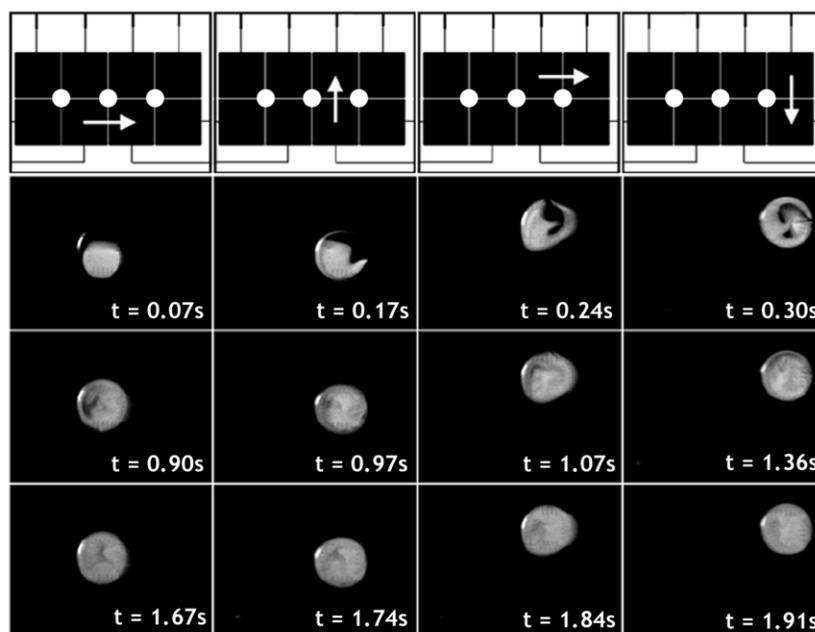
Fig. 9 Pivot points about which a droplet moves in a 2 × 4 array mixer (top row) and time-lapsed images of 2 × 4 electrode mixing at 16 Hz.
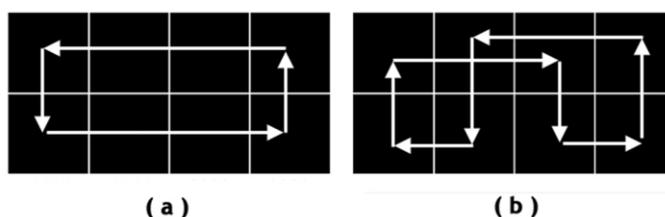
Fig. 10 Two possible paths a coalesced droplet could take in a 2 × 4 array mixer.
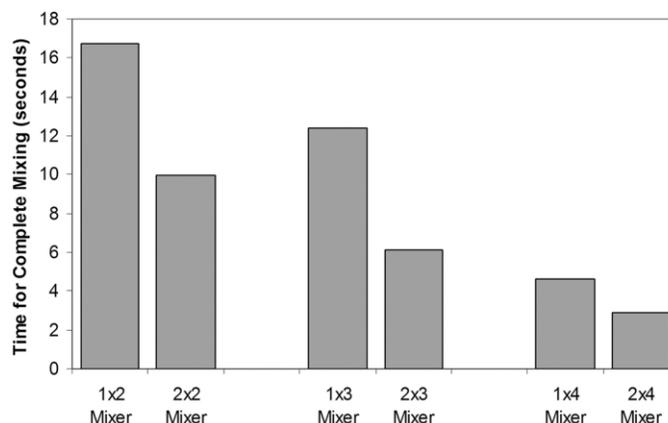
Fig. 12 Complete mixing times for various $1 \times N$ and $2 \times N$ array mixers at 16 Hz.

turn of a droplet occurs about a different pivot point as opposed to multiple turns per pivot point with the $2 \times N$ mixers. We observed that the mixing was much slower compared to the 2×4 array mixer using this scheme.

Summary of results

Fig. 12 shows a graph comparing the various linear-array mixers with their two-dimensional array counterparts. We see that mixing times are improved nearly two-fold by the addition of a second dimension (*i.e.* additional pivot points). Furthermore, we see that mixing times are also reduced by increasing the number of electrodes (*i.e.* additional translation steps). Table 1 shows the complete list of the various rapid droplet mixers studied in this paper.

4 Conclusions

In order to achieve rapid mixing for high-throughput micro-fluidic systems, the effects of varying aspect ratios in linear array mixing were first studied. Ratios were varied from 0.2 to 0.66, with an optimal ratio of 0.4 producing the best results, and a ratio of 0.2 producing the worst. For an aspect ratio of 0.2, we presented a split-and-merge mixer that takes advantage of the ability to perform droplet splitting at low aspect ratios. Two 800 nl droplets at a switching frequency of 16 Hz using this scheme were completely mixed within 1.7 seconds. This simple split and merge mixer demonstrates the feasibility of employing droplet splitting for mixing. For systems with larger aspect ratios (>0.2), the optimal aspect ratio of 0.4 was used to study methods to eliminate the effects of flow-reversibility. The results indicate that although these effects can be eliminated using a simple 2×2 electrode array mixer, mixing performed worse than a four electrode linear array mixer. By increasing the number of pivot points about which a droplet can rotate, mixing rates were improved. Mixing was further enhanced by increasing the number of translational steps between each pivot point. The fastest mixing time for two 1.4 μl droplets was 2.9 seconds using the 2×4 electrode array mixer operating at 16 Hz.

While there are many combinations of moving, splitting, and merging droplets, we have only presented a representative sample for each case. More complex mixing schemes which employ droplet splitting are possible and need to be studied. Three dimensional mixing schemes which would move droplets out of plane by vertical actuation to enhance mixing also need

be explored. The effect of absolute scaling into the picoliter regime needs to be studied.

References

1 P. Paik, V. K. Pamula, M. G. Pollack and R. B. Fair, Electrowetting-based droplet mixers for microfluidic systems, *Lab Chip*, 2003, **3**, 28–33.
2 M. A. Burns, B. N. Johnson and D. T. Burke, An integrated nanoliter DNA analysis devices, *Science*, 1998, **282**, 484–487.
3 K. Hosokawa, T. Fujii and I. Endo, Handling of picoliter liquid samples in a poly(dimethylsiloxane)-based microfluidic device, *Anal. Chem.*, 1999, **71**, 4781–4785.
4 M. G. Pollack, A. D. Shenderov and R. B. Fair, Electrowetting-based actuation of liquid droplets for microfluidic applications, *Lab Chip*, 2002, **2**, 96–101.
5 M. G. Pollack, R. B. Fair and A. D. Shenderov, Electrowetting-based actuation of liquid droplets for microfluidic applications, *Appl. Phys. Lett.*, 2000, **77**(11), 1725–1726.
6 M. Washizu, Electrostatic actuation of liquid droplets for micro-reactor applications, *IEEE Trans. Ind. Appl.*, 1998, **34**, 732.
7 J. Lee, H. Moon, J. Fowler, T. Schoellhammer and C. J. Kim, Electrowetting and electrowetting-on-dielectric for microscale liquid handling, *Sens. Actuators, A: Phys.*, 2002, **95**(2–3), 259–268.
8 T. B. Jones, M. Gunji, M. Washizu and M. J. Feldman, Dielectrophoretic liquid actuation and nanodroplet formation, *J. Appl. Phys.*, 2001, **89**, 1441–1448.
9 V. K. Pamula, P. Paik, J. Venkatraman, M. G. Pollack and R. B. Fair, Microfluidic electrowetting-based droplet mixing, *Proc. IEEE MEMS*, 2001, 8–10.
10 J. Fowler, H. Moon and C. J. Kim, Enhancement of mixing by droplet-based microfluidics, *Proc. IEEE MEMS*, 2002, 97–100.
11 V. Srinivasan, V. K. Pamula, K. Divakar, M. G. Pollack, J. A. Izatt and R. B. Fair, 3-D Imaging of moving droplets for microfluidics using optical coherence tomography, 2003, *Proceedings of μTAS* (accepted).
12 S. K. Cho, H. Moon and C. J. Kim, Creating, Transporting, Cutting, and Merging Liquid Droplets by Electrowetting-Based Actuation for Digital Microfluidic Circuits, *J. Microelectromech. Syst.*, 2003, **12**(1), 70–80.
13 V. Srinivasan, V. K. Pamula, M. G. Pollack and R. B. Fair, A digital microfluidic biosensor for multianalyte detection, *Proc. IEEE MEMS*, 2003, 327–330.
14 H. Ren, V. Srinivasan and R. B. Fair, Design and testing of an interpolating mixing architecture for electrowetting-based droplet-on-chip chemical dilution, 2003, *IEEE Transducers* (accepted).